Transverse diffusion of Ar^+ and Ar^{2+} in Ar

G. Sejkora,* P. Girstmair, H. C. Bryant,† and T. D. Märk
Institut für Experimentalphysik, Leopold Franzens Universität, A-6020 Innsbruck, Austria
(Received 29 November 1983)

The ratio of the transverse-diffusion coefficient to the mobility determines the transverse Gaussian spreading of a pencil beam of ions pulled through a buffer gas by a uniform electric field. The mathematical basis for this effect is reviewed and a precision apparatus to measure the transverse spread is described. Measurements of the transverse diffusion of Ar^+ and Ar^{2+} in Ar in the pressure range from 0.2 to 0.6 Torr at room temperature for E/N values ranging from 30 to 290 Td are presented and discussed (1 Td$\equiv 10^{-17}$ V cm^2).

I. INTRODUCTION

The irreversible dispersal of an initially confined collection ("swarm") of particles in a static gas in which the mean free path between collisions is small compared with the dimensions of the space in which the observations are made is usually called "diffusion." The history and theoretical underpinnings of the diffusion of charged particles have been well discussed by McDaniel and Mason[1(a)] and Huxley and Crompton.[2] In general, the number density of particles undergoing diffusion as a function of space and time can be characterized in a very precise and orderly way by the diffusion equation, even though the individual particles are undergoing completely uncorrelated and random motions.

When the diffusing particles are ions and a constant electric field is present, we find, excepting cases of "runaway,"[3,4] that the swarm develops a constant drift velocity in the direction of the electric field and that the rate of diffusion becomes anisotropic. We consider here only ion densities so small that the effects of mutual electrostatic repulsion are negligible. The diffusion equation must be modified (see, for example, McDaniel and Mason[1(b)]) by the introduction of a diagonal diffusion tensor, with D_T being the coefficient of transverse (or lateral) diffusion, characterizing the rate of dispersal perpendicular to the applied field, and D_L being the coefficient of longitudinal diffusion characterizing the diffusion along the field. An additional term must be included as well for the drifting of the swarm. If particles are removed or added to the swarm (by reactions with the buffer gas or other reactant gas), we must also include a corresponding term in the modified diffusion equation. In Sec. II we display this diffusion equation and discuss the relevant "steady-state" solutions.

This paper describes in some detail a new method for the measurement of D_T and discusses results for Ar^+ and Ar^{2+} in Ar. A thesis based on this work at an earlier stage was presented by Sejkora,[5] and a preliminary report on measurements on the diffusion of N_2^+ in N_2 has been given.[6]

The strategies used by experimenters in measuring D_T involve studying the variation of the swarm density under controlled conditions for which tractable solutions to the diffusion equation are known, thereby allowing the extraction of D_T. Thus the method used by Townsend[7] and subsequently Skullerud,[8] Rees and co-workers,[9–12] and Stefansson[13] is to sense the transverse spreading of the swarm lateral to the field by directly measuring the current density onto two half-plates as a function of transverse distance (r) from the field axis (z) along which the swarm enters the diffusion region.

Another method is that of McDaniel and coworkers[14–16] in which the variation in axial current density is determined as a function of distance along the direction (z) of the electric field.

A third method is that of Varney *et al.*[17] who measured the variation in the axial current density as a function of the drift velocity (or E/N). We shall have more to say about this technique in Sec. II, in discussing solutions to the diffusion equation.

The method we describe here belongs to the Townsend tradition in that we measure the lateral distribution of the swarm directly. It differs, however, in two important respects from the Townsend method: the current density is sensed at individual points, rather than as integrals over two electrodes, and the particles detected are mass-analyzed to select the particular species we wish to study.

The scientific motivation for undertaking precise measurements of D_T, beyond its intrinsic interest, is that D_T, in conjunction with D_L, is particularly sensitive to the long-range part of the ion-neutral interaction potential, which is difficult to study in other ways.[1(a),18] Specifically, D_T is very sensitive to the large-angle scattering cross section.

In Sec. III we describe the apparatus used in our measurements, which are described in Sec. IV. The results of measurements of Ar^+ and Ar^{2+} diffusing in Ar are presented in Sec. V and discussed in Sec. VI.

II. STEADY-STATE SOLUTIONS TO THE DIFFUSION EQUATION

A. Diffusion equation

The starting point in the analysis of diffusion measurements of ions in a gas under the influence of a uniform field is the modified diffusion equation.[1(a),2] For cylindrical symmetry, we may write

$$\frac{\partial n}{\partial t}=D_L\frac{\partial^2 n}{\partial z^2}+D_T\frac{1}{r}\frac{\partial}{\partial r}r\frac{\partial}{\partial r}n-w\frac{\partial n}{\partial z}-\alpha n\ , \tag{1}$$

where $n\equiv n(r,z,t)$ is the number density of a single species of ions at z,r (axial and radial coordinates, respectively) at time t. α is the rate of loss of these ions per unit time due to reactions with reactants which are assumed to be uniformly dispersed throughout the volume. The diffusion coefficients are functions of the temperature, reduced electric field (electric field E divided by the neutral gas number density N), the kind of ion, and the composition of the buffer gas. w is the drift velocity of the ions through the gas under the influence of a constant, uniform electric field E. Thus

$$w=KE\ , \tag{2}$$

where K is the mobility, which depends upon the same variables as do the diffusion coefficients.

B. The "big-bang" solution

As has been demonstrated by, for example, McDaniel and Mason,[1(a)] the solution to the diffusion equation for a point source of ions located at $z=r=0$ which emits a vanishingly narrow pulse of n_0 ions at time $t=0$, where all boundaries are ignored, is

$$n(r,z,t)=\frac{n_0}{(4\pi t)^{3/2}D_T D_L^{1/2}}\times\exp\left[-\alpha t-\frac{r^2}{4D_T t}-\frac{(z-wt)^2}{4D_L t}\right]. \tag{3}$$

A steady-state solution for the case when the point source emits a steady stream of ions, rather than a singular pulse, can be constructed from the above time-dependent solution as follows. Set

$$n_0=n_0' d\tau_0\ , \tag{4}$$

the number of ions emitted in the time interval $d\tau_0$ at time τ_0, where n_0' is a constant rate (number per unit time). The number density at r,z from such a source that has been emitting for a long time is

$$n(r,z)=\int_{-\infty}^{t} d\tau_0 n(r,z,t-\tau_0)n_0'/n_0\ , \tag{5}$$

where the variable of integration is τ_0, following from Eq. (4).

If we make the substitution $\tau=t-\tau_0$ in Eq. (5), we can write

$$n(r,z)=\int_0^{\infty} d\tau\, n(r,z,\tau)n_0'/n_0\ , \tag{6}$$

where τ is now the variable of integration. Explicitly,

$$n(r,z)=\frac{n_0'\exp(zw/2D_L)}{(4\pi)^{3/2}D_T D_L^{1/2}}\times\int_0^{\infty} d\tau\,\tau^{-3/2}\exp\left[-\frac{\beta}{\tau}-\gamma\tau\right], \tag{7}$$

where $\beta=r^2/4D_T+z^2/4D_L$ and $\gamma=w^2/4D_L+\alpha$.

In Gradshteyn and Ryzhitz[19] we find

$$\int_0^{\infty} x^{\nu-1}e^{-\beta/x-\gamma x}dx=2(\beta/\gamma)^{\nu/2}K_\nu(2\sqrt{\beta\gamma})\ , \tag{8}$$

where K_ν is the Bessel function of imaginary argument. In our case $\nu=-\frac{1}{2}$, for which

$$K_{-1/2}(z)=(\pi/2z)^{1/2}e^{-z}\ . \tag{9}$$

The integral then becomes

$$n(r,z)=\frac{n_0'\beta^{-1/2}}{8\pi D_T D_L^{1/2}}\exp[zw/2D_L-2(\beta\gamma)^{1/2}]\ ,$$

or

$$n(r,z)=\frac{n_0'}{4\pi D_T z}\frac{1}{(1+\epsilon)^{1/2}}\times\exp\left[\frac{zw}{2D_L}[1-(1+\delta)^{1/2}(1+\epsilon)^{1/2}]\right], \tag{10}$$

where $\delta=4D_L\alpha/w^2$ and $\epsilon=r^2D_L/z^2D_T$. For the case where δ and ϵ are small compared with 1, we can write

$$n(r,z)=\frac{n_0'}{4\pi D_T z}\exp\left[-\frac{r^2 w}{4zD_T}-\frac{\alpha z}{w}\right]. \tag{11}$$

This formula may be obtained in a plausible, if not convincing way, suggested by Huxley and Crompton,[2] by putting $D_L=0$ in Eq. (6), which results in the expression

$$n(r,z)=\frac{n_0'}{4\pi D_T w}\int_0^{\infty}\frac{d\tau}{\tau}\exp\left[-\alpha\tau-\frac{r^2}{4D_T\tau}\right]\times\delta(\tau-z/w)\ , \tag{12}$$

giving immediately Eq. (11), where δ is the Dirac δ function.

C. Particle current density

We measure particle current density rather than ion volume density. If the sampling aperture does not unduly distort the drift field in its vicinity, we expect the particle current density j to be related to the ion volume density n by the formula (McDaniel and Mason[1(c)])

$$j=wn-D_L\frac{\partial}{\partial z}n\ . \tag{13}$$

In the case of Eq. (11)

$$j=\left[w+D_L\left[\frac{1}{z}-\frac{r^2 w}{4z^2D_T}+\frac{\alpha}{w}\right]\right]n\ . \tag{14}$$

For present conditions, one can also safely neglect the second term so that

$$j=wn\ . \tag{15}$$

We see, then, that if the quantity $[X^+]$ of Varney *et al.*[17] is interpreted as particle current density, this formulation agrees with their analysis. The analysis of the present data, as we shall see, does not depend (more than a negligible amount) on whether one uses particle current or ion volume density.

D. Basic formula for further analysis

The complete expression for the current of ions arriving at point r,z is obtained by combining Eqs. (10) and (14):

$$j(r,z)=\frac{n_0' w}{4\pi D_T z}\left[1-\frac{\epsilon}{4}+\frac{\delta}{4}+\frac{D_L}{zw}(1-\epsilon)\right]\frac{e^P}{(1+\epsilon)^{1/2}}, \quad (16)$$

where $P=(zw/2D_L)\{1-[(1+\delta)(1+\epsilon)]^{1/2}\}$, with δ and ϵ as defined for Eq. (10). The quantity P, when expanded to second order in δ and ϵ and simplified, becomes

$$P=\left[-\frac{z\alpha}{w}\left[1-\frac{\delta}{4}\right]-\frac{r^2 w}{4D_T z}\left[1-\frac{\epsilon}{4}+\frac{\delta}{2}\right]\right]. \quad (17)$$

Since, even at the most unfavorable conditions [$p=0.1$ Torr, $E/N=20$ Td (1 Td$\equiv 10^{-17}$ V cm^2), $r=3$ mm, $\alpha=1500$ sec^{-1}], we expect ϵ and δ to be less than 0.01, we have ignored them for the rest of the treatment. In principle, although not done here, one can correct the results for the small systematic shifts stemming from this approximation. Note that the influence of α on the r dependence comes only through δ.

With the above approximations, and remembering that the transverse diffusion coefficient D_T in the present method is determined from only the dependence of j upon r, we can take, for our further analysis, the particle current density

$$j(r)=j(0)\exp(-r^2 w/4D_T z), \quad (18)$$

where $j(0)=(n_0' w/4\pi D_T z)\exp(-\alpha z/w)$, and n_0' is the particle current emitted by the source.

E. Modification of formula for a slit source of finite width

Let us now determine the particle current density at point x,y,z from a slit source of length $2a$ and width $2b$ at $z=0$. (See Fig. 1.) If the particle current density from point ξ,η on the source aperture arriving at $x=\xi, y=\eta$ at the detector is $j_0 d\xi d\eta$, then the total particle current density arriving at an arbitrary x and y, assuming j_0 does not depend upon ξ, is given by

$$j(x,y)=\int_{-a}^{a}\int_{-b}^{b} d\xi d\eta\, j_0(\eta) \times\exp\{-\lambda^2[(x-\xi)^2+(y-\eta)^2]\}, \quad (19)$$

where $\lambda^2=w/4D_T z$.

The critical point is that dependences on x and y separate. The integral on η, $I(y)$, we need not evaluate except to note that the source intensity can in fact depend upon η without affecting the distribution of the diffusing ions along the x axis. Thus

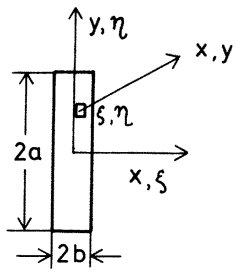

FIG. 1. Geometry of the source slit, looking along the z axis.

$$j(x,y)=I(x)I(y), \quad (20)$$
$$I(x)=\int_{-b}^{+b} d\xi\, e^{-\lambda^2(x-\xi)^2}.$$

For $b^2 \ll 1/\lambda^2$, we can write

$$I(x)=e^{-\lambda^2 x^2}\int_{-b}^{b} d\xi[1+2\lambda^2 x\xi+\lambda^2(2\lambda^2 x^2-1)\xi^2 +O(\xi^3)], \quad (21)$$

or

$$I(x)=2be^{-\lambda^2 x^2}[1+\tfrac{1}{3}\lambda^2 b^2(2\lambda^2 x^2-1)+\cdots]. \quad (22)$$

Since $(\ln 2)^{1/2}/\lambda$ is the half-width at half maximum of the profile, we can neglect any deviation from Gaussian x dependence as long as the slit width is much smaller than that of the profile.

Thus, if the x dependence of the ion current is determined keeping y constant (that is, moving perpendicular to the narrow slit) we can write, with very good approximation,

$$j(x)=j(0)\exp(-x^2 w/4D_T z). \quad (23)$$

This equation, then, is the basis for our analysis of the experimental data.

Note that, although this is unnecessary for our analysis, a further reasonable approximation can be made, namely, that j_0 does not depend upon η and that the slit is very long, so that

$$I(y)=j_0\int_{-\infty}^{\infty} d\eta\exp[-\lambda^2(y-\eta)^2], \quad (24)$$

which gives

$$I(y)=j_0(4\pi D_T z/w)^{1/2}. \quad (25)$$

Thus in this case we can give an explicit expression for $j(0)$,

$$j(0)=\frac{I_0}{2a}(w/4\pi D_T z)^{1/2}\exp(-\alpha z/w), \quad (26)$$

where I_0 is the ion current passing through the entrance slit.

III. APPARATUS

A. Overview

Figure 2 presents a schematic view of the essential apparatus used in the measurement of D_T/K. The key elements are the ion source IQ which can be translated laterally, normal to the entrance slit I with a precision stage S, the ion diffusion region D in which a very uniform, variable electric field can be maintained, the exit aperture E fixed on the axis of symmetry, and the quadrupole mass filter QMF which can be tuned to pass only the desired ion species into the channeltron detector C. The metal used is nonmagnetic stainless steel. In what follows we shall give more specific details. An earlier brief description has been also given by Sejkora *et al.*[20,21]

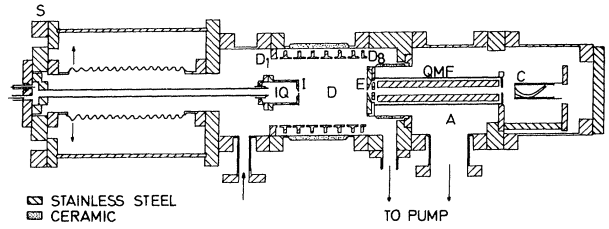

FIG. 2. Schematic view of the transverse diffusion apparatus, showing essential details. See Sec. III.

B. Gas inlet system

Special care was taken so that the gases used in the experiment were of very high purity. For this reason the gas inlet and mixing system of glass and stainless steel can be baked at 300 °C and can be pumped to a high vacuum. Separate spectrographic quality gases or gas mixtures at different pressures can be fed into the ion source and diffusion drift region; the working pressure (0.1—1 Torr) in these regions is measured with capacitance gauges. The Ar used for the measurements described in this paper has impurity levels of less than 5 ppm. In this case the source and the drift space were always kept the same pressure. The high vacuum is measured with an ionization gauge.

C. Ion source

Different ion sources can be interchangeably attached to the ion-source mounting stage with its associated gas and electrical feed-throughs. The source for these measurements is based on α-particle emission. It follows an earlier conception by Crompton and Elford[22] and has been described in detail by Hilchenbach[23] and briefly by Sejkora *et al.*[20,21] Since a detailed paper on this source is planned, only the more relevant features will be described here. A cross section through the longitudinal axis of the source is displayed in Fig. 3. The electrical connections are shown in Fig. 4.

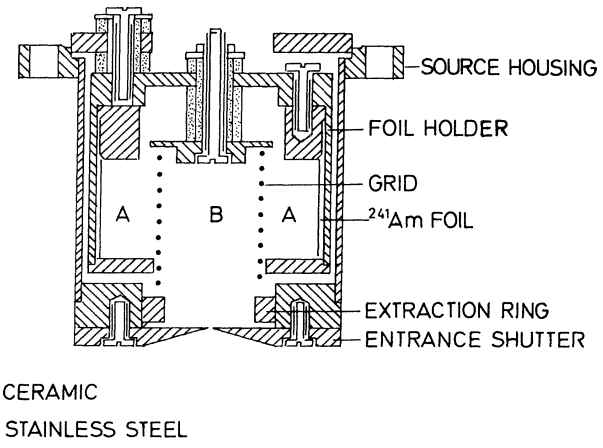

FIG. 3. Schematic view of the ion source. Ionization within the source is produced by Townsend avalanches initiated by α particles from the ^{241}Am foil.

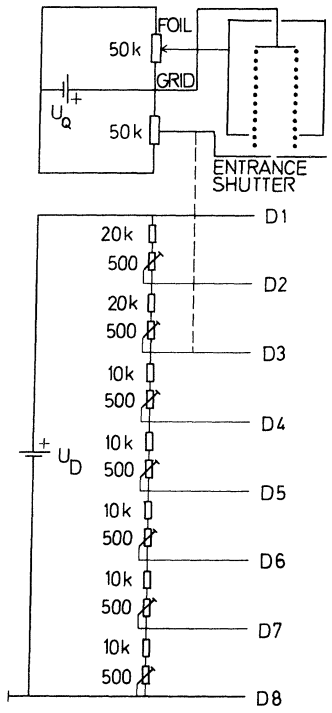

FIG. 4. Schematic diagram of electrical connections.

The source operates as follows, best understood by referring to Fig. 3. Alpha particles (5.5 MeV) from the 9.7×10^7 Bq (2.6 mCi) ^{241}Am foil enter region *A*, where the gas pressure is typically 0.3 Torr. The potential is adjusted (150—250 V) so that Townsend avalanches occur in the radial field in *A*, thereby greatly enhancing the ionization occurring in the gas. The electrons produced in region *A* then enter the nearly field-free region *B* where ions are produced by electron impact, as well as by the original α particles. Approximately 2% of the resulting ions are extracted through the entrance slit with the help of the potential U_{GE} (typically 70 V) applied to the entrance slit shutter. Since the half-life of ^{241}Am is $\sim$460 years,[24] the current output from this source is quite steady, if other conditions are maintained.

The properties of this source which are especially important for our measurements are (1) high stability for ion currents even below 10 pA, (2) working pressures above 0.1 Torr, and (3) no temperature gradients.

D. Source displacement

The ion-source mount is attached to a dovetail stage which can be driven by a precision screw to provide carefully controlled translation perpendicular to the axis of symmetry of the drift tube. The dovetail mechanism prevents any tilting of the source mount. Bearing surfaces are ground flat to 0.001 mm. The stepping motor, which is computer controlled, operates at a frequency of 50 Hz. The displacement of the entrance slit, mounted on the source holder, can be controlled with an accuracy of at least 0.01 mm. As can be seen in Fig. 2, the vacuum seal between the dovetail and the drift chamber is formed by stainless-steel bellows.

E. The entrance slit

The ions enter the diffusion region from the ion source under the influence of the extraction potential U_{GE}, discussed above. The entrance slit formed by two knife edges of stainless steel, and whose length $2a = 20$ mm, is adjusted to have a precise width of $2b = 0.2$ mm.

F. The diffusion region

The diffusion region consists of a cylindrical drift tube 161 mm long and 114 mm in diameter as seen in Fig. 2. The uniform electric field is applied through a series of eight "drift rings" whose potential differences are maintained by a chain of resistors with 500-Ω trimmers, across a doubly stabilized, voltage-regulated power supply, as shown in Fig. 4. As demonstrated by Albritton,[25] such a configuration of drift rings with constant potential differences results in a very uniform electric field. In our case, with a center-to-center spacing of the drift rings of 23 mm, an inter-ring gap of 3 mm, and an inside diameter of the rings of 114 mm, it can be shown[5] that a constant-field region is thereby produced such that in a cylinder 80 mm in diameter, centered on the axis of symmetry, the largest field deviation at any point is no larger than 1.4% of the average field. Deviations within a cylinder of 40 mm diameter, centered within the larger one, are only 0.01%. However, when the cylindrical source is inserted into this uniform field, severe distortion occurs. This distortion is compensated for as follows. The entrance shutter is maintained at the same potential as the third drift ring, as the two have the same axial position; the coupling is indicated by the dotted line in Fig. 4. The first two drift rings, D_1 and D_2, are maintained with a larger potential difference than the others. By a semi-empirical means, using He^+ in He, as well as by direct computation, one can demonstrate that, if the inter-ring gap potential for D_1 and D_2, and D_2 and D_3 is maintained at 2.0 times the inter-ring gap potential for the remaining rings, a reasonably uniform field results. This compensation is accomplished by adjusting resistors R_1 and R_2 to 20 kΩ. The other resistors in the chain are 10 kΩ. Further discussion of the field problem is given under Sec. IV B 4.

The drift tube can routinely be baked out under high vacuum at 300 °C in order to reduce possible contaminants in the buffer gas. For measurements of the diffusion constant, buffer gas pressures ranging from 0.1 to 1 Torr are maintained via a feedback loop. For the present measurements, the drift chamber pressure was monitored with a precise capacitance manometer.

G. The exit aperture

As with the entrance slit, special care must be taken with the exit aperture to insure that the current density measurement not be distorted by inhomogeneous fields and contaminants. The exit aperture, a circular hole 0.15 mm in diameter, is machined from stainless steel. The surface of the exit shutter was machined as flat and scratch-free as possible, with the edges of the circular hole almost knifelike (the edge thickness is 0.05 mm) to minimize transition losses.[26]

Great care was taken to insure that the exit shutter was free of surface contamination. The exit shutter, although electrically isolated to allow the measurement of the total ion current, is maintained at ground potential as is the eighth drift ring D_8.

H. The mass-analyzed detection system

Ions passing through the exit aperture from the diffusion region into an analyzer region A (Fig. 2), where the pressure is 10^{-6} Torr, are accelerated by an extraction electrode (typically 50 V) into a quadrupole mass filter. The potential difference between the quadrupole bias and the exit shutter (typically 30 V) determines the kinetic energy of the ions entering the mass filter, as the kinetic energy of ions in the drift tube is much smaller. The ions transmitted by the mass filter enter a Channeltron detector C, whose entrance aperture is biased at -3 kV, where current pulses are formed and passed on for electronic analysis.

I. The data-acquisition system

A thorough discussion of the microprocessor-controlled data acquisition is presented by Sejkora.[5] At the heart of the system is a microcomputer whose central processing unit is the Intel 8080 chip. Operator access to the system is through a visual display terminal. Working storage is a 48-kbyte RAM (1 kbyte = 1024 × 8 binary digits; RAM is random access memory); data storage is upon "mini floppy disks" with a storage capacity of 100 kbyte per disk through a floppy disk drive.

Since the ion source with the stepping motor and its control logic reside at a substantial positive potential, while the control electronics are kept at ground, it is necessary to optically couple the stepping motor control logic to the computer interface carrying instructions to the stepping motor.

IV. DATA ANALYSIS

A. Determination of D_T/K

At a given E/N and for a specified set of operating conditions, we have the raw data on a run over the ion density profile for a number of distances from the axis of symmetry of the diffusion chamber. The data for such a run consist of a set of displacements p_i (typically 8 to 10) with a corresponding set of current measurements I_{ij} (typically 5 to 10) for each p_i. For each i, an average I_i is computed along with its standard deviation σ_i. Figure 5 shows a typical ion density profile for Ar^+ in Ar after these operations have been performed. The solid line through the points is the result of fitting to Eq. (23). The value of the quantity D_T/K is extracted from the best fit.

B. Fitting the model to the profile

As we have seen in Sec. II, to a very good approximation, the current density profile is expected to have the

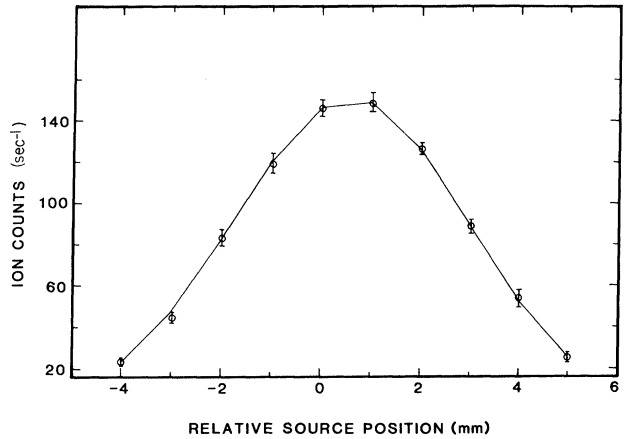

FIG. 5. Typical ion density profile for Ar^+ in Ar. Solid line joins fitted points.

form given by Eq. (23) when the physics involved can be described by Eq. (1). By fitting our data to the model, then, we can check our hypothesis of simple diffusion and extract as well, from the best fit, the value of the quantity D_T/K.

Let us rewrite Eq. (23) as

$$I(p_i)=(R/Q)\exp[-(p_i-M)^2/Q^2]\,, \tag{27}$$

where M is introduced to include the possibility of an offset to the $p_i=0$ point from the axis of the apparatus. Here

$$Q^2=4zD_T/KE$$

and, if Eq. (26) were applicable, for example,

$$R=(I_0/2\sqrt{\pi}a)\exp(-\alpha z/w)\,.$$

A fitting of the function given by Eq. (27) is accomplished by adjusting the parameters Q, R, and M to minimize χ^2, defined as (typically)

$$\chi^2(Q,R,M)=\sum_{i=1}^{n}[I_i-I(p_i)]^2/\sigma_i^2\,. \tag{28}$$

The errors shown for our measurements are based on the standard deviation on the fit for Q, which is taken to be the change in Q that increases χ^2 by 1 above its minimum (best-fit) values. The minimum values of χ^2 obtained by this method are quite consistent with the validity of the putative form of the results given by Eq. (27).

C. Systematic errors

1. Backgrounds

Normally no background is encountered under the Gaussian profile of diffusing particles at the detector. The presence of background would be evident when the mass spectrometer is detuned or if the ion source is turned off. However, the fitting program has the capability of subtracting a background from the data in instances when a background is discovered.

2. Parameter measurements

Uncertainties in the drift distance z and the electric field are less than 1%. The buffer gas pressure was monitored using a capacitance gauge, with a feedback loop to hold the drift pressure constant at the desired value. Although the gauge and its associated electronics were temperature-stabilized, some drift in the zero-point setting occurs, which was observed by periodically evacuating the chamber. For this reason, one expects that the pressure of the drift region was uncertain in these measurements, in a random way from point to point, by approximately ±3%.

3. Space-charge effects

In order to insure that the broadening of the ion density profile was not unduly enhanced by mutual repulsion among the ions, a study of apparent D_T/K was made as a function of source current. The results of this study, for $p\sim0.3$ Torr and $E/N\sim140$ Td, are displayed in Fig. 6. Since the currents used in making the actual D_T/K measurements lie between 1 and 10 pA, space-charge effects evidently play no role. (See also discussion in Ref. 11.)

4. Drift field

As mentioned in Sec. III F above, the presence of the metal ion source housing in the drift region produces distortions which must be corrected. Compensation for these distortions was made by increasing the potentials applied to drift rings D_1 and D_2. The values for the intergap potential difference were determined by an empirical method: The apparent value of D_T/K for He^+ in He at 50 Td and 0.674 Torr was measured as a function of the ratio of the inter-ring gap potential differences between D_1 and D_2, and D_2 and D_3 (kept the same) to that of the gap potentials between the remaining (also kept the same). When this ratio was very near 2.0, the measured value of D_T/K agreed with that predicted by Sinha *et al.*,[27] which we judged was likely to be a reasonably precise and accurate value. (See also Waldman *et al.*[28])

A computer model[29] of the drift field indicates that the electric field at the exit slit may be 3% less than the field near the source. Simple considerations lead us to estimate that our measurements may be systematically 3% too

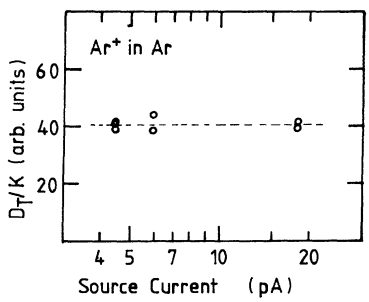

FIG. 6. Check for possible space-charge effects.

large, as a result of this field variation. This correction has not been applied to the data.

V. RESULTS FOR Ar^+ AND Ar^{2+} in Ar

A. Ar^+ in Ar

Figure 7 displays our present data taken at 298 K. The error bars along the vertical axis reflect the results of error analysis discussed above, but do not include any estimate of the possible effects of systematic errors. The data are also tabulated in Table I. There is no apparent systematic pressure effect; the scatter among the experimental points then gives us an intrinsic estimate of the experimental error. The earlier (smoothed) data of Varney *et al.*[17] are included for comparison.

B. Ar^{2+} in Ar

Figure 8 displays measurements of Ar^{2+}, which are listed in Table II, taken under the same circumstances as Ar^+. Since the ratio of ion currents Ar^{2+} to Ar^+ coming from the ion source was small, these data are based on lower counting rates than those for Ar^+. Measurements below 50 Td were especially difficult. Repeated measurements at 50 Td, given in Table II, give an internal estimate of the experimental (nonsystematic) error. The standard deviation of 0.6 mV is somewhat larger than the errors arising from the Gaussian fit alone. There is no obvious pressure dependence.

VI. DISCUSSION

In contrast with the mobility measurements of Ar^+ and Ar^{2+} in their parent gas[30–32] which show a very similar functional dependence on E/N (over the E/N range considered here the reduced mobility of Ar^{2+} is very nearly a constant 1.06 $cm^2/V\,sec$ more than the reduced mobility for Ar^+; at 200 Td that of Ar^{2+} is twice that of Ar^+) our measurements of D_T/K, when plotted versus E/N, Figs.

TABLE I. Ar^+ on Ar.

E/N (Td)	D_T/K (mV)	p (Torr)	χ^2
30	27.3±0.4	0.39	8.1
40	28.0±0.3	0.57	3.0
50	29.1±0.5	0.39	3.7
60	29.7±0.3	0.57	2.3
	30.7±0.2	0.39	3.9
69	30.3±0.3	0.57	1.9
70	31.3±0.3	0.39	0.8
	28.0±0.4	0.33	7.2
90	32.6±0.5	0.33	4.7
100	32.0±0.3	0.39	4.4
	32.5±0.3	0.25	0.9
110	34.5±0.4	0.33	6.3
130	36.4±0.4	0.33	3.7
150	38.8±0.4	0.33	5.0
	37.5±0.3	0.33	6.9
	37.4±0.5	0.24	8.9
170	39.1±0.5	0.33	3.3
	41.2±0.3	0.24	4.0
190	42.7±0.5	0.24	2.2
	43.3±0.4	0.33	6.4
210	42.8±0.4	0.24	2.7
	42.9±0.3	0.21	9.3
230	44.9±0.4	0.21	5.1
	46.5±0.6	0.24	2.1
250	45.7±0.4	0.16	5.3
270	47.1±0.5	0.16	5.0
290	48.3±0.4	0.16	3.5

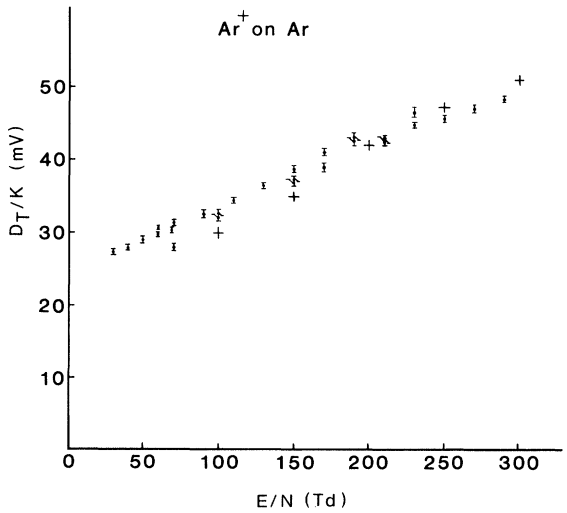

FIG. 7. D_T/K for Ar^+ in Ar vs E/N. Crosses are data of Varney *et al.* (Ref. 17).

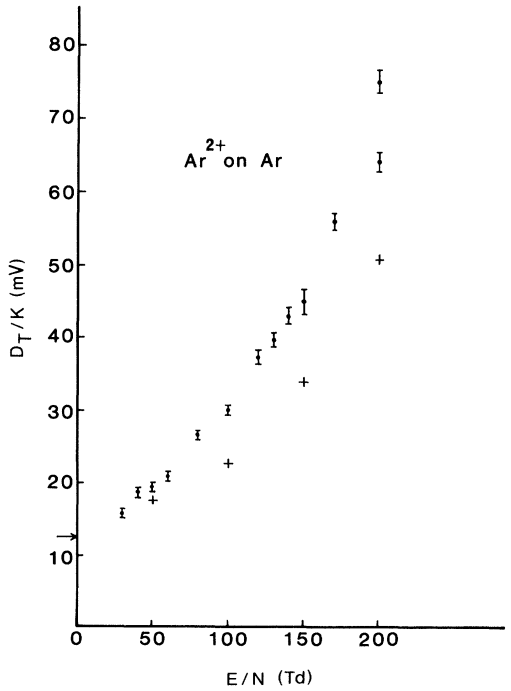

FIG. 8. D_T/K for Ar^{2+} in Ar vs E/N. Crosses are data of Varney *et al.* (Ref. 17). Data points at 200 Td are not included in Fig. 9 or tabulated as we regard them as unreliable.

TABLE II. Ar^{2+} on Ar.

E/N (Td)	D_T/K (mV)	p (Torr)	χ^2
30	15.9±0.4	0.57	6.0
40	19.2±0.3	0.57	4.0
	18.3±0.4	0.39	1.9
50	19.6±0.3	0.76	3.2
	18.4±0.3	0.67	3.8
	19.4±0.4	0.57	2.7
	20.5±0.4	0.57	3.4
	19.9±0.3	0.48	8.0
	19.7±0.4	0.39	1.6
	19.8±0.4	0.30	6.3
60	21.0±0.4	0.57	4.4
80	26.9±0.5	0.48	6.1
100	30.2±0.7	0.25	1.7
120	37.6±0.8	0.26	4.3
130	39.8±0.9	0.25	1.0
140	43.1±1.2	0.26	2.5
150	46.0±1.1	0.26	2.7
	43.7±0.9	0.25	3.7
170	56.0±1.0	0.76	0.9

7 and 8, seem to display a qualitatively different behavior. This apparent qualitative difference between the transverse diffusion measurements, however, decreases significantly when we plot the same data versus w^2, as seen in Fig. 9. In this plot, we see the two charge states are almost parallel; the difference in curvature seen in Figs. 7 and 8 is almost entirely removed. w is calculated using the tabulated reduced mobilities K_0 of Beaty:[31]

$$w = 269 K_0 (E/N) . \tag{29}$$

If (E/N) is in Td, w is in cm/sec.

When the data are fitted with a function of the form

$$D_T/K = a + bw^2 , \tag{30}$$

we see that the slopes are indeed similar, as seen in Table III. This apparent similarity between the two data sets at first is perplexing, because as Varney *et al.*[17] point out, one expects the charge exchange cross sections, especially,

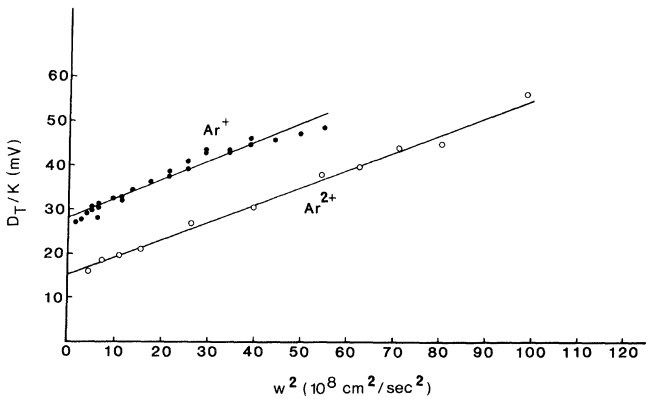

FIG. 9. D_T/K for Ar^+ (solid circles) and Ar^{2+} (open circles) in Ar vs w^2.

TABLE III. Fits of the function $D_T/K = a + bw^2$ to the experimental data and corresponding derived values for R.

Reaction	Range E/N (Td)	a (mV)	b (mV sec^2/cm^2)	R
$Ar^+ + Ar$	up to 90	26.8	5.67×10^{-9}	0.345
	up to 190	26.9	5.22×10^{-9}	0.311
	all	28.0	4.24×10^{-9}	0.242
$Ar^{2+} + Ar$	all	15.3	3.93×10^{-9}	0.531

to be very different for the two charged states. It is a relief, then, to discover that the difference reappears when we consider the theoretical interpretation of the constants in Eq. (30).

From very basic considerations[1(a)] one can demonstrate that

$$a = kT/q , \tag{31}$$

a relationship known variously as the "Nernst-Townsend" or "Einstein" relation.

The usual interpretation of b by experimentalists (e.g., Alger *et al.*,[12] Varney *et al.*[17]) is as an approximate expression due to Wannier[33] and discussed by Skullerud,[18]

$$b = (1 + m/M) R (4m/M + 3R)^{-1} M/q , \tag{32}$$

where M and m are the masses of the buffer gas and ion, respectively, and R is identified as the ratio of the viscosity cross section to the momentum-transfer cross section, σ_2/σ_1. The values of R, calculated from this expression, are also given in Table III. We see that because of the factor of 2 in q in Eq. (32), similar b values result in very different values for R. As can be seen, our measurements agree in form with those made earlier in Innsbruck by Varney *et al.*[17] Since the method of these earlier workers involved an extrapolation to zero E/N to establish proper normalization as well as a deliberately large attenuation of the ions in water vapor, which was taken to be constant over the E/N range, we regard the two sets of measurements to be in reasonable agreement. The agreement on the Ar^+ seems to be excellent, whereas the values of D_T/K for Ar^{2+} at the larger (E/N)'s are divergent. Our results do not agree with the earlier measurement of Skullerud.[8]

VII. CONCLUSION

Our measurements confirm the remarkably different behavior of D_T/K for the two positive ions of argon in argon observed by Varney *et al.*,[17] using a different experimental technique.[34,35] In the parametrization discussed by Skullerud we find $\sigma_2/\sigma_1 = 0.242$ and 0.531 for Ar^+ and Ar^{2+}, respectively. The large qualitative difference seen in the behavior of D_T/K versus E/N for the two charged states is mostly explained by the large, almost constant difference in mobility between the two, so that when plotted versus energy the two curves are almost parallel.

ACKNOWLEDGMENTS

We wish to thank our colleagues in this Institute for their continued help. The contributions of Dr. H. Helm of SRI International, Menlo Park, CA, and M. Hesche, Innsbruck, are gratefully acknowledged. This work is supported by the Fonds zur Förderung der wissenschaftlichen Forschung (Austria). One of us (H.C.B.) gratefully acknowledges support by a Fulbright fellowship and by the U. S. Department of Energy, Division of Chemical Sciences. The apparatus described in the present study was constructed by G.S. in partial fulfillment of the requirements for a Ph.D. at the University of Innsbruck.

*Present address: Institut für Textilchemie und Textilphysik, Achstr. 1, A-6850 Dornbirn, Austria.

†Permanent address: Department of Physics and Astronomy, The University of New Mexico, Albuquerque, NM 87131.

[1](a) E. W. McDaniel and E. A. Mason, *The Mobility and Diffusion of Ions in Gases* (Wiley, New York, 1973); (b) *ibid.*, p. 3; (c) *ibid.*, p. 76.

[2]L. G. H. Huxley and R. W. Crompton, *The Diffusion and Drift of Electrons in Gases* (Wiley, New York, 1974).

[3]S. L. Lin, I. R. Gatland, and E. A. Mason, J. Phys. B 12, 4179 (1979).

[4]F. Howorka, F. C. Fehsenfeld, and D. L. Albritton, J. Phys. B 12, 4189 (1979).

[5]G. Sejkora, Dissertation, Universität Innsbruck, 1982.

[6]G. Sejkora and T. D. Märk, Chem. Phys. Lett. 97, 123 (1983).

[7]J. S. Townsend, Proc. R. Soc. London, Ser. A 80, 207 (1908).

[8]H. R. Skullerud, *Proceedings of the Seventh International Conference on Phenomena in Ionized Gases, Belgrade, 1965,* edited by B. Perovic and D. Tosić (Gradjevinska Knjiga, Belgrade, Yugoslavia, 1966).

[9]I. A. Fleming, R. J. Tunnicliffe, and J. A. Rees, J. Phys. D 2, 551 (1969).

[10]I. A. Fleming, R. J. Tunnicliffe, and J. A. Rees, J. Phys. B 2, 780 (1969).

[11]D. R. Gray and J. A. Rees, J. Phys. B 5, 1048 (1972).

[12]S. R. Alger, T. Stefansson, and J. A. Rees, J. Phys. B 11, 3283 (1978).

[13]T. Stefansson, in Proceedings of the Third International Swarm Seminar, Innsbruck, edited by W. Lindinger *et al.*, 1983 (unpublished).

[14]J. T. Moseley, R. M. Snuggs, D. W. Martin, and E. W. McDaniel, Phys. Rev. Lett. 21, 873 (1968).

[15]T. M. Miller, J. T. Moseley, D. W. Martin, and E. W. McDaniel, Phys. Rev. 173, 115 (1968).

[16]J. T. Moseley, R. M. Snuggs, D. W. Martin, and E. W. McDaniel, Phys. Rev. 178, 240 (1969).

[17]R. N. Varney, H. Helm, E. Alge, H. Störi, and W. Lindinger, J. Phys. B 14, 1695 (1981).

[18]H. R. Skullerud, J. Phys. B 9, 535 (1976).

[19]I. S. Gradshteyn and I. M. Ryzhik, *Tables of Integrals, Series and Products,* corrected and enlarged edition (Academic, New York, London, 1980).

[20]G. Sejkora, M. Grössl, H. Helm, M. Hilchenbach, M. T. Elford, W. Lindinger, and T. D. Märk, in Proceedings of the Third Symposium Atomic Surface Physics, Maria Alm, 1982 (unpublished).

[21]G. Sejkora, M. Hilchenbach, M. T. Elford, and T. D. Märk, Europhys. Conf. Abs. 6D, 143 (1982).

[22]M. T. Elford (private communication).

[23]M. Hilchenbach, Diplomarbeit, Universität Innsbruck, 1982.

[24]W. Kunz and J. Schintlmeister, *Tabellen der Atomkerne, Teil I* (Akademie, Berlin, 1959), p. 1062.

[25]D. L. Albritton, thesis, Georgia Institute of Technology, 1967.

[26]M. Grössl, M. Langenwalter, H. Helm, and T. D. Märk, J. Chem. Phys. 74, 1728 (1981).

[27]S. Sinha, S. L. Lin, and J. N. Bardsley, J. Phys. B 12, 1613 (1969).

[28]M. Waldman, E. A. Mason, and L. A. Viehland, Chem. Phys. 66, 339 (1982).

[29]M. Hesche, Diplomarbeit, Universität Innsbruck, 1984.

[30]M. A. Biondi and L. M. Chanin, Phys. Rev. 94, 910 (1954).

[31]E. C. Beaty, *Proceedings of the Fifth International Conference on Ionization Phenomena in Gases, München, 1961* (North-Holland, Amsterdam, 1961), Vol. 1, p. 183; see H. W. Ellis, R. Y. Pai, E. W. McDaniel, E. A. Mason, and L. A. Viehland, At. Data Nucl. Data Tables 17, 196 (1976).

[32]R. Johnsen and M. A. Biondi, Phys. Rev. A 18, 989 (1978).

[33]G. H. Wannier, Bell Syst. Techn. J. 32, 170 (1953).

[34]For a more detailed discussion of the presently introduced radial ion distribution method (see also an earlier study by Rees and Alger, Ref. 35) see the recent review by E. Märk and T. D. Märk, in *Swarms of Ions and Electrons in Gases,* edited by W. Lindinger, T. D. Märk, and F. Howorka (Springer, Wien, 1984).

[35]J. A. Rees and B. A. Alger, Proc. IEEE 126, 356 (1979).